Anomalous magnetism in decagonal $Al_{69.8}Pd_{12.1}Mn_{18.1}$

D. Rau,* J. L. Gavilano, Sh. Mushkolaj, C. Beeli, M. A. Chernikov, and H. R. Ott
Laboratorium für Festkörperphysik, ETH Zürich, 8093 Zürich, Switzerland
(Received 14 February 2003; revised manuscript received 5 June 2003; published 7 October 2003)

We report the results of measurements of ^{27}Al and ^{55}Mn NMR spectra, the related spin-lattice relaxation rates, and the dc magnetic susceptibility of the stable decagonal quasicrystal $Al_{69.8}Pd_{12.1}Mn_{18.2}$. The temperature variation of the magnetic susceptibility $\chi(T)$ reveals that the Mn ions carry only an effective magnetic moment of approximately $2\mu_B$, and confirms a spin-glass-type freezing of the Mn moments at $T_f = 12$ K. The NMR spectra reveal two partially resolved lines for the ^{27}Al-nuclei, indicating that there are two different sets of environments for the Al-sites. The integrated intensity of the Mn line in the spectra suggests that about half of the Mn ions carry no magnetic moment. Below 50 K, and upon decreasing the temperature, the ^{27}Al NMR linewidth w and the spin-lattice relaxation rate T_1^{-1} both grow with an increasingly negative slope, as it is often observed and interpreted as a critical ''slowing down'' of magnetic moments in systems approaching a spin-glass transition. Various features, such as a broad maximum in $T_1^{-1}(T)$ and a slope change in the $w(\chi)$ plot, both around 120 K, suggest a gradual reduction of the number of Mn moments with decreasing temperature below 120 K.

DOI: 10.1103/PhysRevB.68.134204 PACS number(s): 61.44.Br, 76.60.−k, 75.50.Lk

I. INTRODUCTION

Since the discovery of quasicrystalline systems by Shechtman *et al.* in 1982 (first published[1] in 1984), substantial progress in the understanding of quasicrystalline structures has been made.[2–4] Quasicrystalline structures are characterized by a high degree of atomic order, resulting in well-defined x-ray and electron-diffraction peaks, but they lack translational periodicity. This complicates the understanding of the electronic structure and hence of some important physical properties. The unusual electronic transport properties are often traced back to the formation of a pseudogap in the excitation spectrum at the Fermi level.[5,6] The nonperiodicity of the crystal lattice is the reason for special features in the temperature dependence of the thermal conductivity, reflecting a general type of Umklapp scattering.[6–9] The quasiperiodic atomic arrangement is expected to also influence the magnetic features of quasicrystals (QC's), and in recent years, studies of magnetic properties of QC's have been in the focus of a number of research projects. While the initial studies were mainly performed on metastable Al-Mn QC's,[10,11] a lot of progress has been made since then in preparing stable high-quality ternary QC's with local magnetic moments in alloy systems such as Al-Pd-Mn or Al-Mn-Ge. Depending on structure and stoichiometry, these QC's exhibit ferromagnetism,[12] diamagnetism,[13] paramagnetism,[14,15] or spin-glass phenomena.[16–18] Other intensively investigated families of magnetic QC's include Al-Cu-Fe and Al-Co-Ni alloys,[19] and the more recently synthesized quasicrystalline compounds containing rare-earth (RE) ions, such as RE-Mg-Zn with well localized $4f$-electron moments.[20–23]

Several studies of the *d*-electron magnetism of Mn in icosahedral samples of Al-Pd-Mn have been motivated by the early discovery of the stable icosahedral *i*-Al-Pd-Mn phase. In spite of the above-mentioned variety of magnetic properties found in these QC's, they seem to exhibit the common feature of only a small fraction of the manganese ions carrying a magnetic moment.[14,17] In some cases this fraction even seems to decrease with decreasing temperature.[14] Theoretical studies and band-structure calculations aimed at explaining the phenomenon that only a fraction of the Mn ions carries a magnetic moment,[24] and to relate it to the Hume-Rothery-type pseudogap in the electronic spectrum around the Fermi level.[25]

In comparison with the icosahedral Al-Pd-Mn alloys, the situation is less clear for decagonal Al-Pd-Mn alloys. For the latter, a larger number of sites have been predicted to carry a moment which, however, is smaller than the Mn moment established in icosahedral compounds.[25] The present work reports the results of measurements of the dc magnetic susceptibility and of ^{27}Al- and ^{55}Mn-NMR studies of the decagonal QC *d*-$Al_{69.8}Pd_{12.1}Mn_{18.1}$. From our results we infer that, in the paramagnetic state and above 100 K, about half of the Mn atoms are nonmagnetic, and that magnetic and nonmagnetic Mn ions are distributed equally over the crystal at very short distances. The data further indicate that the fraction of Mn moments may even decrease upon reducing the temperature below 100 K. Finally, we confirm the previously reported spin-glass transition at $T_f = 12$ K.[26]

II. THE SAMPLE

A metastable icosahedral sample of Al-Pd-Mn was obtained by spinning a melt of the stoichiometric composition of the decagonal phase $Al_{69.8}Pd_{12.1}Mn_{18.1}$ onto a fast turning (30 m/s), water cooled Cu wheel. Annealing the resulting tapes with the icosahedral phase for 100 h at about 820 °C transforms them into polycrystalline flakes of the stable decagonal phase.[27] Decagonal Al-Pd-Mn has a columnar structure arranged on a two-dimensional quasiperiodic lattice. The translational period of length $d = 12.56$ Å is built up by two different types of layers: a puckered layer *P* and a flat layer *F*.[3] The ratio of Al in *P* to Al in *F* is approximately 2:1; for Mn this ratio is about 1:8.[2] Within the quasicrystalline layers the longest distance between two identical coordination polyhedra is of the order of 3 nm.

 ©2003 The American Physical Society

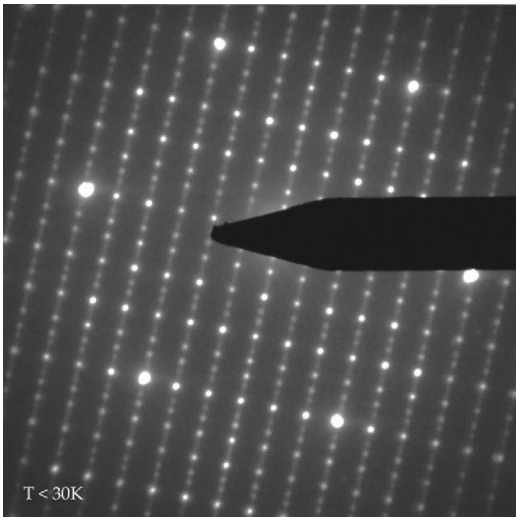

FIG. 1. Selected area electron-diffraction (SAED) picture of *d*-Al-Pd-Mn at 30 K.

High-resolution transmission electron microscopy confirmed that our sample consists of polycrystalline *d*-$Al_{69.8}Pd_{12.1}Mn_{18.1}$ with no linear phason strains. Selected area electron diffraction from room temperature down to below 30 K proved the high perfection of the decagonal symmetry in the planes and the periodicity along the *c* axis (see Fig. 1). Scanning electron microscopy sets the upper limit of the admixture of a second phase, i.e., $Al_{11}(Mn,Pd)_4$ on the surface of the backside of the tapes, to about 1%, and confirms a high homogeneity.

III. EXPERIMENTAL RESULTS AND THEIR ANALYSIS

A. Magnetic susceptibility

We measured the dc-susceptibility $\chi(T)$ of *d*-$Al_{69.8}Pd_{12.1}Mn_{18.1}$ with an (rf-superconducting quantum interference device) magnetometer between 340 K and 2 K, and at different magnetic fields between 50 G and 5.5 T. Figure 2 shows the inverse susceptibility $1/[\chi(T)-\chi_0]$ measured at 500 G between 5 K and 350 K. As may be seen in the lower inset of Fig. 2, field-cooled and zero-field-cooled (ZFC) data differ below $T_f \approx 12$ K. There is a well-defined maximum for the ZFC $\chi(T)$ at T_f. This behavior confirms a spin-glass-type freezing of the Mn moments, previously claimed from the analysis of ac susceptibility and specific-heat results measured on the same sample.[26] Above 120 K, $\chi(T)$ may be approximated by $\chi(T)=C/(T-\Theta)+\chi_0$ with

$$C = N_A c p^2 \frac{\mu_B^2}{3k_B}, \tag{1}$$

where N_A is Avogadro's number, *c* the concentration of magnetic ions, and *p* their effective moment. The susceptibility data in the temperature range between 120 K and 350 K are best approximated with the parameters $C=0.544$ emu/mol, $\Theta=-20$ K, and $\chi_0=-2.45\times10^{-8}$ emu/g.[28]

The negative paramagnetic Curie temperature Θ indicates a predominant antiferromagnetic coupling between the Mn *d*

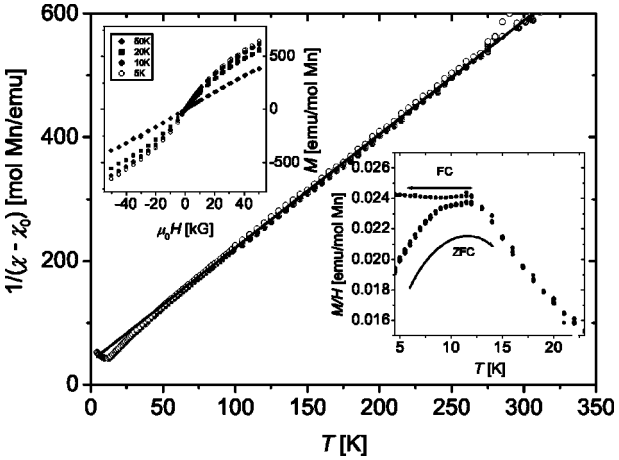

FIG. 2. The inverse dc susceptibility $\chi(T)$ after subtracting a constant negative offset per mol of Mn in an applied field of 500 G. The solid line represents the high-temperature Curie-Weiss fit. The lower inset displays the dc susceptibility below 24 K. Below $T_f = 12$ K the zero-field-cooled data deviate from the temperature-independent field-cooled data. The upper inset displays the magnetization $M(H)$ at several temperatures.

moments. The Curie constant *C* implies that $p\sqrt{c}=(2\pm0.1)\mu_B$. As may be expected, this is not compatible with the assumption that all Mn ions adopt a well-defined and identical ionic configuration. If we assume, for example, localized Mn moments, our result for $\chi(T)$ implies a concentration of only $16.5\pm0.5\%$ of Mn^{3+}, or $12.5\pm0.5\%$ of Mn^{2+}. Distinct deviations of $\chi(T)$ from the Curie-Weiss behavior below 60 K (see main frame of Fig. 2) signal precursor effects of the spin-glass freezing of the Mn moments.

Below 50 K the susceptibility is field dependent below 5 T. The upper inset in Fig. 2 displays the magnetization $M(H)$ measured at various temperatures. The expected hysteresis of $M(H)$ in the spin-glass state due to ''memory effects'' is too small to be visible on the scales of Fig. 2.

B. NMR spectra

We recorded ^{27}Al and ^{55}Mn NMR spectra between room temperature and 8 K and at the frequencies of 21, 25, 30, 58, and 70 MHz, using standard $\pi/2$-τ-π spin-echo sequences. Figure 3 shows NMR spectra recorded at 96 K, with an excitation frequency of 24.97 MHz but different pulse sequences (see below). The NMR signal is distributed over a wide range of resonant fields from 2.15 to 2.45 T. The prominent peak near 2.25 T represents the central ^{27}Al Zeeman transition $(1/2 \leftrightarrow -1/2)$. The broad distribution of quadrupolar wings is a generic feature of QC's.[29] The vertical dotted line in Fig. 3 indicates the position of the resonance of ^{27}Al nuclei in an aqueous $AlClO_3$ solution at room temperature and 24.97 MHz, which is used as a reference signal. The solid lines represent the results of a computer simulation of the spectra which is described below.

The ^{27}Al central transition is very broad, almost a factor of 10 broader than expected from considering the second-order quadrupolar perturbation of the Zeeman line and than

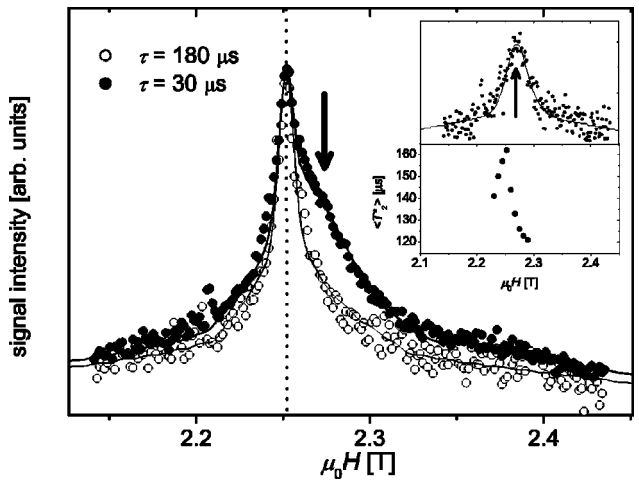

FIG. 3. ^{27}Al and ^{55}Mn NMR spectra of *d*-AlPdMn at 24.97 MHz and 96 K with $\tau=30$ μs and $\tau=180$ μs. The arrow indicates the center of line II which is also indicated by an arrow in the upper inset. The upper inset displays the difference between the spectra at 180 μs and 30 μs, after taking T_2^* effects into account. The solid line in the inset is the contribution of line II to the fit of the total line in the main frame. The lower inset presents the average spin-spin relaxation rate $\langle T_2^* \rangle$ at different fields. The excess signal at 2.207 T again arises from the ^{63}Cu nuclei of the measurement coil. For the definition of T_2^* see text.

the analogous signals observed for the case of the nonmagnetic Al-Pd-Re compounds.[29] The linewidth increases with decreasing temperature. We argue that this signal consists of two partially resolved contributions representing the central transitions of Al nuclei located in either of two distinctly different local environments. One of the contributions, denoted as line I in Fig. 4, has very small or zero line shift, while the other, denoted as line II in Fig. 4, exhibits a relatively large and *T* dependent negative shift.

In order to confirm this conjecture, we have looked for and found appreciable differences in the spin-spin relaxation for the ^{27}Al nuclei that were allocated to different environments. This was achieved by changing τ in the $\pi/2$-τ-π echo

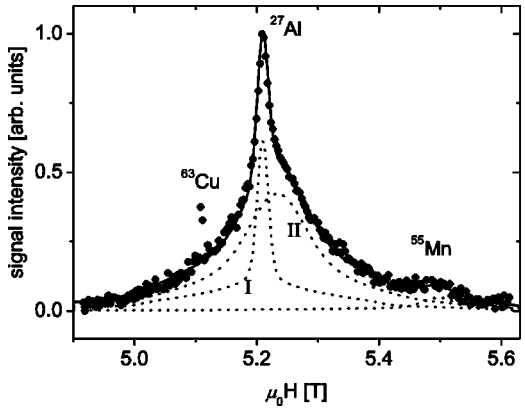

FIG. 4. ^{27}Al and ^{55}Mn NMR spectrum of *d*-AlPdMn at 57.8 MHz and 101 K. The solid line represents a fit to the data, the dotted lines indicate the individual contributions of line I, line II, and the Mn signal.

sequence. Figure 3 displays two spectra recorded at 24.97 MHz and 96 K with two different values for τ. The spectrum with $\tau=30$ μs shows a distinct shoulder on the high-field side while in the spectrum with $\tau=180$ μs this feature is clearly absent. In the upper inset of Fig. 3 we display the difference of the two spectra after taking into account the spin-echo lifetime T_2^* ($1/T_2^*=1/T_1+1/T_2\approx 1/T_2$). These effects affect both line I and line II, which experience a suppression of signal intensity due to transverse relaxation processes. The loss of signal due to these processes has been taken into account by weighing factors obtained from a fit of $Ae^{(-2\tau+d_2)/T_{2,\mathrm{I}}^*}+Be^{(-2\tau+d_2)/T_{2,\mathrm{II}}^*}$ to the echo intensity as a function of τ, with d_2 as the duration of the π pulse. The thus obtained difference of the two spectra then reveals a clear manifestation of line II. The solid lines in the inset as well as in the main frame display the results of computer simulations, briefly discussed below. We conclude that the agreement between the experimental data and the calculated curves provides strong evidence for the existence of two different types of environments for the Al nuclei, giving rise to signals I and II, respectively.

Support for our claims is obtained from the results of our computer simulations of NMR spectra measured in a wide range of *T*, *H*, and τ values. The NMR frequency of a nucleus depends on the local magnetic field and on the local electric-field gradient at the position of the nucleus, such that

$$\nu=\nu_{\mathrm{L}}-\nu_{\mathrm{Q}}\left(m-\frac{1}{2}\right)\frac{3\cos^2\theta-1}{2}, \tag{2}$$

where ν_{L} and ν_{Q} denote the Larmor and the quadrupolar frequencies, respectively, *m* is the *z* component of the upper nuclear spin state of the transition, and θ is the angle between the principal axis of the field gradient and the local magnetic field at the position of the nucleus. We assumed that the Larmor frequencies ν_{L} obey a Gaussian distribution whose width *w* is caused by a (*T* dependent) distribution of shifts, centered around ν_0. Our previous attempts for fitting the—much simpler—^{27}Al spectra of nonmagnetic icosahedral quasicrystals of the Al-Pd-Re family were successful when choosing the quadrupolar frequency ν_{Q} to be uniformly distributed between some hundred kilohertz and a few megahertz. In the simulated ^{27}Al spectra of the present work, this distribution of ν_{Q} ranges from 200 kHz to 2 MHz. The experimental spectra were successfully fitted by assuming two different sets of environments, characterized by two Gaussian distributions with different widths w_{I} and w_{II} spread around two different central frequencies $\nu_{0,\mathrm{I}}$ and $\nu_{0,\mathrm{II}}$. The distribution of ν_{Q} cited above was assumed to be the same for both environments. Figure 4 shows the calculated three contributions to the total spectrum, i.e., line I and line II of ^{27}Al in the two different environments, and the signal originating from nuclei of nonmagnetic Mn ions (discussed below). The distribution of angular orientations of the local quadrupolar axes was assumed to be random, because we used a polycrystalline sample.

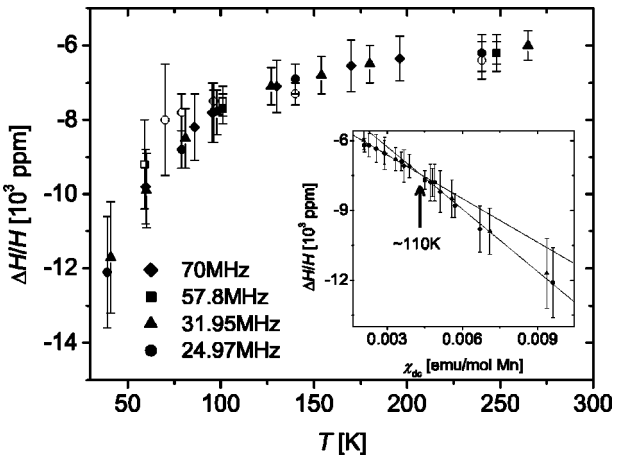

FIG. 5. Temperature dependence of the relative ^{27}Al line shifts $\Delta H/H$ of line II in *d*-AlPdMn at various fields. The open symbols represents the values obtained from the difference of the lines recorded with $\tau=30$ μs and $\tau=180$ μs, respectively. The closed symbols are values obtained from fits to the spectra. The inset shows the line shifts plotted vs the dc susceptibility. There is a slight change of slope at ≈ 110 K, indicated by the two lines and the arrow.

C. NMR line shifts and widths

We determined the shift ΔH_{II} of line II by means of, computer simulations of signals obtained with $\tau=30$ μs and also by subtracting the spectrum monitored with a long τ from that recorded with a short τ, both at the same temperature, of course. Figure 5 shows the relative line shift $\mathrm{K_{II}}=\Delta H_{\mathrm{II}}/H$ of line II as a function of temperature. The open symbols indicate the values obtained by subtraction and the closed symbols correspond to values obtained by computer simulations. The absolute line shifts ΔH scale linearly with field and can be expressed by

$$K=\frac{\Delta H}{H}=K_{\mathrm{ce}}+K_{\mathrm{mag}}(T), \tag{3}$$

where K_{ce} is a temperature-independent contribution, which in our case is much larger in magnitude than those found in nonmagnetic quasicrystals.[14,29,30] Temperature-independent NMR line shifts can be caused by a variety of processes, however, K_{ce} of line II is too large to be attributed to typical chemical shifts or to quadrupolar effects. Therefore, one is tempted to associate K_{ce} with the paramagnetism of the conduction electrons. In common metals this contribution, the Knight shift, is positive, but in our case K_{ce} is negative. A negative and temperature-independent line shift cannot be caused by conduction electrons originating from the Al *s* and *p* shells but may be due to itinerant electrons originating from the Mn *d* shell.[31,32] The Pd *d* band is full and therefore these states are not expected to contribute significantly to the resonance shift. Such an interpretation is compatible with recent experimental results concerning the electronic structure of Al-Pd-Mn quasicrystals.[33]. Nevertheless, the origin of the negative Knight shifts, also found in other quasicrystals, is still an open question. For line I the relative shift *K* is also negative but less than 100 ppm. The existence of two distinct lines with different shifts therefore strongly suggests that the conduction electron density at the ^{27}Al nuclei is not uniform. At some Al sites, which contribute to the intensity of line II, a substantial conduction electron density provides a strong coupling of the Al nuclei to the Mn magnetic moments. At other Al-sites, which contribute to line I, the conduction-electron density is reduced and the coupling to the Mn moments is weaker.

$K_{\mathrm{mag}}(T)$, only clearly observed for line II, exhibits a Curie-Weiss-type behavior in the whole temperature range covered by the data shown in Fig. 5. The paramagnetic Curie temperature $\theta=-6$ K is in fair agreement with the value obtained from fits to the susceptibility. The inset of Fig. 5 displays the line-shift data plotted versus the dc susceptibility measured in different fields. It confirms that $K_{\mathrm{mag}}(T)$ may be written as

$$K_{\mathrm{mag}}(T)=A\chi(T). \tag{4}$$

The proportionality constant *A* is a measure of the average coupling strength of the ^{27}Al nuclear spins to the Mn magnetic moments. For metals, *A* is usually written as[32]

$$A=\frac{1}{\mu_B N_A}H_{\mathrm{eff}}, \tag{5}$$

with H_{eff} as the hyperfine field from each aligned Bohr magneton. N_A is Avogadro's number. In our case, where only a fraction *c* of the Mn ions is magnetic and because the molar susceptibility is calculated per total Mn content, Eq. (5) has to be changed to

$$A=\frac{1}{\mu_B c N_A}H_{\mathrm{eff}}. \tag{6}$$

In spite of the large errorbars, our data suggest that there are two temperature regimes with different values of *A*, below and above ≈ 110 K. This change may simply reflect a reduction of the fraction of magnetic Mn moments *c*. However, other processes leading to a change in the hyperfine coupling cannot be ruled out.

The widths of both lines increase with decreasing temperature and therefore give a clear indication that they are both of magnetic origin. Also line I is much broader than the central ^{27}Al line in other Al-Pd-Mn compounds,[14] suggesting that likewise the nuclei contributing to line I experience some interaction with the magnetic Mn moments and that all, magnetic and nonmagnetic Mn ions as well as the Al nuclei contributing to both the observed signals, are finely dispersed in the bulk of the sample. At this point we focus our attention on line II, where the influence of the Mn moments is particularly pronounced. In Fig. 6 the temperature dependence of the ratio $w_{\mathrm{II}}/\nu_{\mathrm{irrad}}$, where w_{II} is again the width of line II and ν_{irrad} the corresponding irradiation frequency, is plotted for four different irradiation frequencies, i.e., four different average applied fields. Since all the data fall onto a single curve, it follows that the linewidth scales with the irradiation frequency, or, equivalently, with the applied magnetic field and, therefore, must be of magnetic origin. The enhancement with decreasing temperature occurs with increasingly nega-

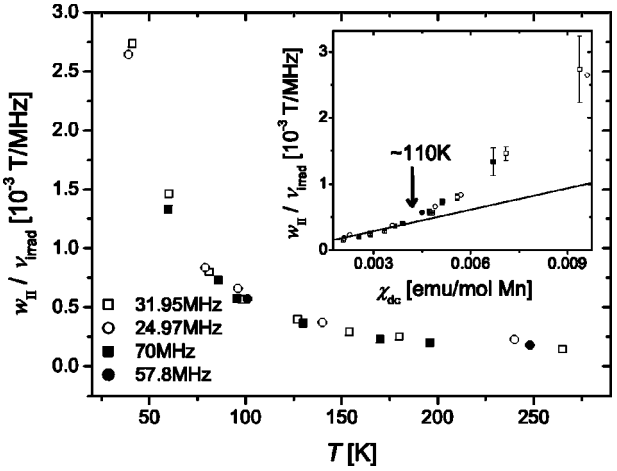

FIG. 6. Temperature dependence of the width of line II divided by the irradiation frequency ν_{irrad}. The inset shows the same ratio plotted vs the dc susceptibility. There is a pronounced change of slope at ≈ 110 K, indicated by the arrow. The solid line fits the data at elevated temperatures.

tive slope. The inset of Fig. 6 displays the same data plotted versus the dc susceptibility measured in similar fields. The width of line II originates from a distribution of shifts of the ^{27}Al nuclei around an average shift. The slope of that curve therefore is a measure of the width of the distribution of the site dependent coupling strengths $A(\mathbf{r})$ between the Al nuclear spins of line II and the Mn moments, with respect to the total magnetic susceptibility, which is mainly due to localized Mn moments. It shows a pronounced change at ≈ 110 K. Such a slope change could be induced by a reduction of the number of magnetic Mn ions, leading to a reduced increase in the susceptibility. Likewise, a change in the hyperfine coupling could also account for these slope changes, but as we argue in the following paragraph, this is an unlikely scenario.

The NMR spectra recorded at a chosen frequency reveal some additional intensity at a field where one expects the ^{55}Mn signal at zero shift. This is most clearly seen near 5.5 T in Fig. 4. Since the hyperfine-field coupling of the Mn moment to the nucleus of the same ion is through the core polarization, which is of the order of -100 kG/μ_{B} for Mn,[32] even a small moment on a Mn ion would shift its resonance frequency out of our experimental window. Therefore the observed signal intensity in our spectra must originate from the nonmagnetic Mn atoms. We compared the total integrated Mn spin-echo intensity obtained from the spectra recorded at 70 MHz, where the Mn signal is clearly resolved, with the integrated intensity of the two Al lines. Taking into account the stoichiometric composition of *d*-Al-Pd-Mn, and the intrinsic NMR sensitivities of ^{55}Mn and ^{27}Al, we conclude from the chemical composition that the total intensity of the Mn signal above and below 100 K, respectively, is only $35\pm 15\%$ and $50\pm 15\%$ of what is expected considering the chemical composition. If we assume that the missing intensity represents the nuclei of the magnetic Mn ions, we may conclude that in the corresponding temperature ranges only a fraction of $65\pm 15\%$ or $50\pm 15\%$ of Mn ions carry a magnetic moment. This decrease of the Mn intensity in the NMR spectra is independent of any possible change of the hyperfine coupling at the Al-sites and it strongly supports our interpretation that the percentage of magnetic Mn below 100 K is reduced. Considering the effective moment of $\tilde{p}=(2\pm 0.1)\mu_B$, deduced from the dc molar susceptibility data with respect to the total Mn content, we estimate that the average effective moment per magnetic Mn ion is $p\approx 3\mu_B$, if we assume that 50% of the Mn ions actually carry a moment. This number is not compatible with any of the possible ionization states of Mn, which would lead to $p=4\mu_B$ for Mn^{4+}, $p=5\mu_B$ for Mn^{3+}, and $p=5.9\mu_B$ for Mn^{2+}.

D. NMR spin-lattice relaxation rate

We measured the spin-lattice relaxation rate T_1^{-1} of line I from room temperature down to 15 K in three different applied fields. The values of T_1 were extracted from fits to the nuclear magnetization recovery $m(t)$, which was first destroyed using a long comb of rf pulses, followed by a variable delay t and a spin-echo sequence $\pi/2$-τ-π with a long $\tau=180$ μs. In this manner it is possible to identify exclusively the spin-lattice relaxation rate related to line I. Using shorter values of τ in these measurements leads to changes in $m(t)$ which, in our view, results in less reliable values of T_1. According to standard NMR theory, the signal intensity of the central line of a spin $I=5/2$ nucleus relaxes such that[34]

$$1-m(t)/m(\infty)=0.4762e^{-15t/T_1}+0.2667e^{-6t/T_1}+0.2571e^{-t/T_1}. \quad (7)$$

Even for line I alone, there is no distinct single Al site, but rather a variety of sites leading to a distribution of T_1's. Since the details of the distribution of T_1's are not known, we simply model $m(t)$ by replacing the exponentials by stretched exponential functions:[35]

$$1-m(t)/m(\infty)=0.4762e^{-15(t/T_1)^{\beta}}+0.2667e^{-6(t/T_1)^{\beta}}+0.2571e^{-(t/T_1)^{\beta}}. \quad (8)$$

Figure 7 displays an example of a magnetization recovery at a relatively low temperature and the corresponding best fit to the data using Eq. (8). With an increasing pulse separation τ in the echo sequence the exponent β converges to an approximate value of 0.9. Therefore, in the subsequent analysis we set $\beta=0.9$. As may be seen in the inset of Fig. 7, the T_1 also values turned out to vary with τ but to reach a constant value for $\tau\geqslant 180$ μs. Therefore, we fixed τ to 180 μs for all the measurements of T_1 discussed below.

In Fig. 8 we present $T_1^{-1}(T)$ obtained from fitting the magnetization recovery data, measured at three different fields of 5.2 T, 2.25 T, and 1.85 T with $\tau=180$ μs, to Eq. (8). The $T_1^{-1}(T)$ plot exhibits a broad maximum centered around 120K. This maximum is very unusual and has—to our knowledge—never been seen in $T_1^{-1}(T)$ of any other quasicrystalline compound. The spin-lattice relaxation rate usually contains three contributions,

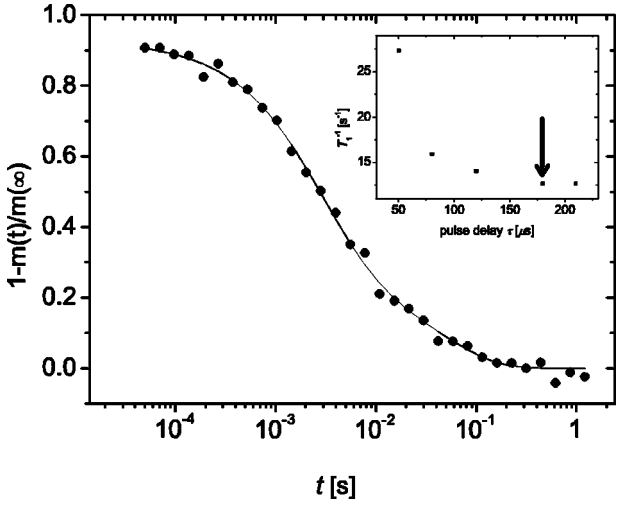

FIG. 7. Magnetization recovery curve related to line I at 57.8 MHz and 24.5 K. The solid line represents a fit to Eq. (8). The inset displays how $T_1^{-1}(68\ \mathrm{K})$ saturates with increasing τ. The arrow marks $\tau = 180\ \mu$s, the pulse delay that was used in our measurements.

$$T_1^{-1} = T_{1,\mathrm{ce}}^{-1} + T_{1,\mathrm{mag}}^{-1} + T_{1,\mathrm{q}}^{-1}. \tag{9}$$

The total relaxation is characterized by $T_{1,\mathrm{ce}}^{-1}$, due to conduction electrons, $T_{1,\mathrm{mag}}^{-1}$ reflecting the relaxation due to the paramagnetic centers, and $T_{1,\mathrm{q}}^{-1}$ capturing the quadrupolar relaxation. In a simple metal, $T_{1,\mathrm{ce}}^{-1}$ is known to vary linearly with temperature. In quasicrystals the relaxation due to itinerant electrons depends on the shape of the density of states at the Fermi level and thus on the shape of the pseudogap. A power law or polynomial increase of the spin-lattice relaxation rate with rising temperature is expected.[5,29] It may be seen in Fig. 8 that above 175 K the T dependence of the spin-lattice relaxation rate may well be dominated by conduction electrons and that they still contribute significantly to the total T_1^{-1} in the crossover regime around 120 K. However, $T_{1,\mathrm{ce}}^{-1}$ cannot account for the maximum at 120 K, unless

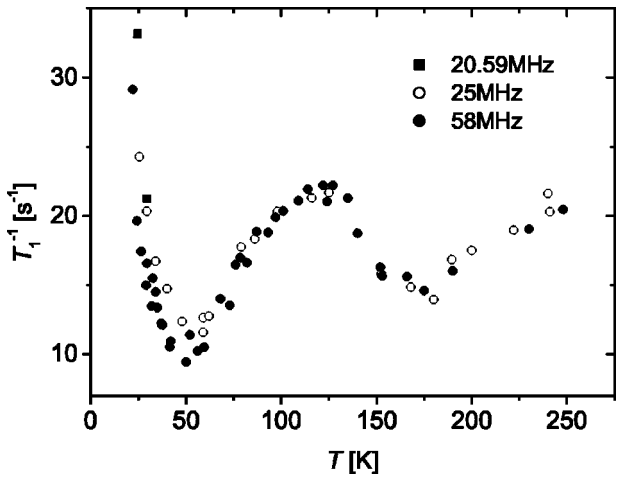

FIG. 8. Spin-lattice relaxation rate $T_1^{-1}(T)$ for line I between 25 and 250 K.

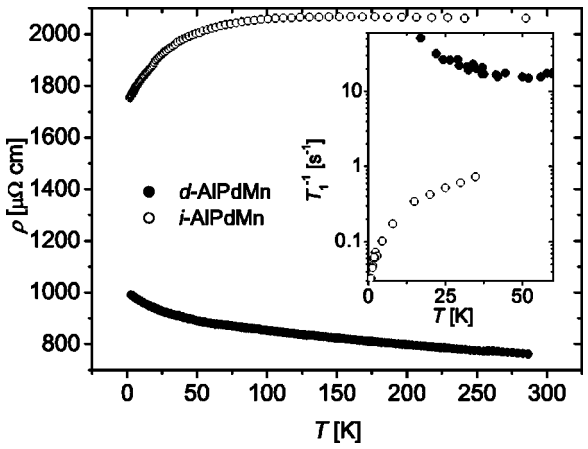

FIG. 9. Zero-field electrical resistivity $\rho(T)$ of *d*-Al-Pd-Mn compared to $\rho(T)$ of *i*-Al-Pd-Mn (Ref. 15). The inset displays $T_1(T)$ of *d*-Al-Pd-Mn at low temperatures in comparison with $T_1(T)$ of the less Mn rich, icosahedral *i*-AlPdMn (Ref. 14).

some anomaly in the electronic excitation spectrum causes the feature at that temperature. Such an anomaly is unlikely because the monotonous variation of the electrical resistivity with temperature, shown in Fig. 9, does not suggest a corresponding feature in the electronic excitation spectrum that would cause the anomaly in T_1^{-1} around 120 K.

Also any substantial contribution of $T_{1,\mathrm{q}}^{-1}$ can be ruled out. The spin-lattice relaxation rate of Al nuclei is larger by more than a factor of 10 in *d*-Al-Pd-Mn than it is in *i*-Al-Pd-Re, where it is still dominated by $T_{1,\mathrm{ce}}^{-1}$ and not by $T_{1,\mathrm{q}}^{-1}$.[5] Hence $T_{1,\mathrm{q}}^{-1}$ in *d*-Al-Pd-Mn is expected to be very small in comparison with other contributions, unless a major change of structure at some temperature occurs in that compound. Results of selected area electron-diffraction (SAED) measurements from room temperature down to below 30 K indicate that no structural changes occur in this temperature regime and therefore it may be concluded that $T_{1,\mathrm{q}}^{-1}$ does not contribute significantly to changes in $T_1^{-1}(T)$.

We are thus left with the second significant term in Eq. (9), i.e., $T_{1,\mathrm{mag}}^{-1}$, which describes the magnetic interactions between the Al nuclear spins and the Mn *d* moments. We note that the values of T_1^{-1} of the icosahedral samples of Al-Pd-Mn with lower Mn concentration[14] are smaller than for the presently investigated material by one order of magnitude (see inset of Fig. 9). With the resistivities of the two compounds being of almost equal magnitude (see Fig. 9), this giant difference in T_1^{-1} is mainly attributed to the larger contribution of $T_{1,\mathrm{mag}}^{-1}$ to the total spin-lattice relaxation rate in the present case. Based on these arguments we suggest that the maximum in $T_1^{-1}(T)$ may be related to $T_{1,\mathrm{mag}}^{-1}(T)$ and that it reflects the previously mentioned reduction of the concentration of magnetic Mn moments below ≈ 100 K.

Below 50 K the spin-lattice relaxation rate displayed in Fig. 8 increases with an increasingly negative slope as T approaches the spin-glass freezing temperature T_f. This behavior is typical for nuclear spins which experience the influence of magnetic moments that undergo a gradual slowing down of their fluctuations. In the present case, the Mn mo-

ments, although predominantly affecting line II, are also felt in the relaxation of the nuclear spins contributing to line I, as the spin-glass transition is approached upon cooling. At high temperatures, the spin-lattice relaxation rate of nonmagnetic nuclei due to paramagnetic centers is given by[36]

$$\frac{1}{T_{1,\mathrm{mag}}} = C\frac{\tau_c}{1+\omega_I^2\tau_c^2}, \tag{10}$$

where C is proportional to the hyperfine-field coupling between the Mn moments and the Al nuclei, τ_c is the correlation time of the Mn moments, and $\omega_I = 2\pi\nu_{0,\mathrm{I}}$ is the Larmor precession frequency of the nucleus under investigation.[37] As T is reduced towards T_f, the moment fluctuations slow down and cause an increase of $T_{1,\mathrm{mag}}^{-1}$ ($\propto\tau_c$), as observed below 50 K. The τ_c-driven increase can be understood by assuming that $\omega^2\tau_c^2$ is still much less than 1, which is implicitly confirmed by the almost H-independent increase of $T_1^{-1}(T)$ below 50 K. Close to T_f, the growing linewidth usually prohibits to extract reliable T_1 values. In our case this is true for $T<20$ K.

IV. SUMMARY

Our susceptibility data and our NMR spectra reveal that at elevated temperatures more than half of the Mn ions in decagonal $Al_{69.8}Pd_{12.1}Mn_{18.1}$ carry a small magnetic moment, giving rise to an average Mn moment $\tilde{p}$ of $2\mu_B$. These moments experience an average antiferromagnetic interaction, leading to a spin-glass freezing at $T_f \approx 12$ K. We presented arguments that the number of these moments is gradually reduced below 100 K. A similar reduction of moments was observed at lower temperatures in *i*-Al-Pd-Mn with a much smaller density of magnetic Mn moments.[14]

The ^{27}Al NMR spectra show two partially resolved lines. Line II is clearly much more influenced by the Mn magnetism. Similar line shapes have been found in very early experiments on Mn-rich metastable Al-Mn quasicrystals,[11] but they could not be resolved into two lines at that time. We argue that the two lines are due to Al on sites in environments favoring the formation of a magnetic moment on the Mn ions (line II) and to Al in an environment, where the Mn moments are quenched (line I). Our results strongly suggest that simple Al-*p*-Mn-*d* hybridization alone may not adequately account for the phenomenon of Mn magnetism in QC's, but that a more subtle, conduction-electron mediated long-range mechanism has to be considered.[24]

We have not yet found an unequivocal interpretation for the broad maximum of T_1^{-1} at 120 K. The same process that leads to that maximum seems to lead to a reduction of the fraction of Mn ions that carry a magnetic moment. Neither a structural transition nor a significant change in the electronic density of states is indicated by SAED and transport measurements, respectively.

ACKNOWLEDGMENTS

We thank René Monnier for fruitful discussions, Roland Wessiken for his help with the temperature-dependent selected area electron diffraction, and Matthias Weller for his assistance in the measurement of the electrical conductivity.

*Electronic address: drau@solid.phys.ethz.ch

[1] D. Shechtman, I. Blech, and J.W. Cahn, Phys. Rev. Lett. **53**, 1951 (1984).
[2] C. Beeli and S. Horiuchi, Philos. Mag. B **70**, 215 (1994).
[3] W. Steurer, T. Haibach, B. Zhang, C. Beeli, and H.-U. Nissen, J. Phys.: Condens. Matter **6**, 613 (1994).
[4] M. Boudard, M. DeBoissieu, C. Janot, G. Heger, C. Beeli, H.-U. Nissen, H. Vincent, R. Ibberson, M. Audier, and J.M. Dubois, J. Phys.: Condens. Matter **4**, 10 149 (1992).
[5] X.-P. Tang, E.A. Hill, S.K. Wonnell, S.J. Poon, and Y. Wu, Phys. Rev. Lett. **79**, 1070 (1997).
[6] K. Giannò, A.V. Sologubenko, L. Liechtenstein, M.A. Chernikov, and H.R. Ott, Ferroelectrics **250**, 249 (2001).
[7] P.A. Kalugin, M.A. Chernikov, A. Bianchi, and H.R. Ott, Phys. Rev. B **53**, 14 145 (1996).
[8] M.A. Chernikov, A. Bianchi, E. Felder, U. Gubler, and H.R. Ott, Europhys. Lett. **35**, 431 (1996).
[9] P.A. Kalugin and A. Katz, Europhys. Lett. **21**, 921 (1993).
[10] M.E. McHenry, D.D. Vvendesky, M.E. Eberhard, and R.C. O'Handley, Phys. Rev. B **37**, 10 887 (1988).
[11] W.W. Warren, H.-S. Chen, and G.P. Espinosa, Phys. Rev. B **34**, 4902 (1986).
[12] Y. Yokoyama and A. Inoue, Mater. Trans., JIM **37**, 559 (1996).
[13] F. Hippert, M. Audier, H. Klein, R. Bellissent, and D. Boursier, Phys. Rev. Lett. **76**, 54 (1996).
[14] J.L. Gavilano, D. Rau, S. Mushkolaj, H.R. Ott, J. Dolinšek, and K. Urban, Phys. Rev. B **65**, 214202 (2002).
[15] J. Dolinšek, M. Klanjšek, T. Apih, J.L. Gavilano, K. Giannò, H.R. Ott, J.M. Dubois, and K. Urban, Phys. Rev. B **64**, 024203 (2001).
[16] H. Fujimaki, K. Motoya, H. Yasuoka, K. Kimura, T. Shibuya, and S. Takeuchi, J. Phys. Soc. Jpn. **60**, 2067 (1991).
[17] M.A. Chernikov, A. Bernasconi, C. Beeli, A. Schilling, and H.R. Ott, Phys. Rev. B **48**, 3058 (1993).
[18] J.C. Lasjaunias, A. Sulpice, N. Keller, J.J. Préjean, and M. de Boissieu, Phys. Rev. B **52**, 886 (1995).
[19] A. Yamamoto, K. Kato, T. Shibuya, and S. Takeuchi, Phys. Rev. Lett. **65**, 1603 (1990).
[20] I.R. Fisher, K.O. Cheon, A.F. Panchula, P.C. Canfield, M. Chernikov, H.R. Ott, and K. Dennis, Phys. Rev. B **59**, 308 (1999).
[21] T.J. Sato, H. Takakura, and A.P. Tsai, Phys. Rev. B **61**, 476 (2000).
[22] K. Giannò, A.V. Sologubenko, M.A. Chernikov, H.R. Ott, I.R. Fisher, and P. Canfield, Mater. Sci. Eng., A **294–296**, 715 (2000).
[23] S. Wessel, A. Jagannathan, and S. Haas, cond-mat/0209405v1 (unpublished).
[24] G.T. de Laissardiere and D. Mayou, Mater. Sci. Eng., A **294–296**, 621 (2000).
[25] J. Hafner and M. Krajčí, Phys. Rev. B **57**, 2849 (1998).
[26] M. A. Chernikov, C. Beeli, E. Felder, S. Büchi, and H. R. Ott (unpublished).
[27] C. Beeli, P. Stadelmann, R. Lück, and T. Gödecke, in *Proceedings of the 5th International Conference on Quasicrystals* (ICQ), ed-

ited by C. Janot and R. Mosseri (World Scientific, Singapore, 1995), Vol. 5.

[28] A careful analysis of our susceptibility data between T_f and 100 K suggests a reduction of the Curie constant to 0.510 emu/mol between 60 K and 100 K, but this temperature interval is, of course, too narrow to draw any reliable conclusion. Below 60 K the shape of $\chi^{-1}(T)$ is dominated by precursor effects of the spin-glass transition.

[29] J.L. Gavilano, B. Ambrosini, P. Vonlanthen, M.A. Chernikov, and H.R. Ott, Phys. Rev. Lett. **79**, 3058 (1997).

[30] T. Apih, M. Klanjšek, D. Rau, and J. Dolinšek, Phys. Rev. B **61**, 11 213 (2000).

[31] A.M. Clogston, V. Jaccarino, and Y. Yafet, Phys. Rev. **134**, A650 (1964).

[32] G. C. Carter, L. H. Bennett, and D. J. Kahan, *Metallic Shifts in NMR* (Pergamon, Oxford, 1977).

[33] M. Erbudak, A. Hensch, J. Keller, B. Roessner, and A.R. Kortan, J. Electron Spectrosc. Relat. Phenom. **120**, 47 (2001).

[34] A. Narath, Phys. Rev. **162**, 320 (1967).

[35] We found good agreement between Eq. (8) and magnetization recoveries obtained by computer simulations of a collection of ensembles with different T_1.

[36] A. Abragam, *Principles of Nuclear Magnetism* (Oxford Science Publications, Oxford, 1994).

[37] Equation (10) is a high-temperature approximation where the correlations among the paramagnetic moments are neglected (Ref. 36).